Single-Molecule Investigations of RNA Dissociation

Nicola H. Green, Philip M. Williams, Omar Wahab, Martyn C. Davies, Clive J. Roberts, Saul J. B. Tendler, and Stephanie Allen

Laboratory of Biophysics and Surface Analysis, School of Pharmacy, University of Nottingham, University Park, Nottingham, United Kingdom

ABSTRACT Given the essential cellular roles for ribonucleic acids (RNAs) it is important to understand the stability of three-dimensional structures formed by these molecules. This study aims to investigate the dissociation energy landscape for simple RNA structures via atomic-force-microscopy-based single-molecule force-spectroscopy measurements. This approach provides details on the locations and relative heights of the energy barriers to dissociation, and thus information upon the relative kinetic stabilities of the formed complexes. Our results indicate that a simple dodecamer RNA helix undergoes a forced dissociation process similar to that previously observed for DNA oligonucleotides. Incorporating a UCU bulge motif is found to introduce an additional energy barrier closer to the bound state, and also to destabilize the duplex. In the absence of magnesium ions a duplex containing this UCU bulge is destabilized and a single, shorter duplex is formed. These results reveal that a bulge motif impacts upon the forced dissociation of RNA and produces an energy landscape sensitive to the presence of magnesium ions. Interestingly, the obtained data compare well with previously reported ensemble measurements, illustrating the potential of this approach to improve our understanding of RNA stability and dissociation kinetics.

INTRODUCTION

The RNA molecule plays a fundamental role in some of the most highly conserved cellular processes, demonstrating a versatility of form and function that is not seen for DNA (Saenger, 1984). RNA can relay genetic information to the ribosome for translation as well as acting as a catalyst at the center of this ribosome. In addition, certain RNAs can fold to form catalytic ribozymes, analogous to enzymes, which assist in RNA processing events whereas others facilitate in specific RNA, DNA, or protein interactions. Many of these roles are largely determined by the complex and specific three-dimensional structures adopted by functional RNA.

When predicting the three-dimensional structures of RNA molecules it is often possible to assign a number of putative structures to one sequence, with current predictions often being based upon an understanding of the thermodynamic and/or kinetic stabilities of a range of potential structures. An improved knowledge of the forces and barriers that control the kinetic stabilities of such structures would thus be valuable to this process, from both a biological and theoretical point of view.

Unlike proteins, whose secondary structures usually depend on the global amino acid sequence, RNA molecules are currently thought to assemble in a hierarchical manner. As a result, RNA exhibits a modular structure with individual structural motifs demonstrating independent characteristics (Saenger, 1984; Brion and Westhof, 1997; Moore, 1999). This has facilitated, in previous theoretical and experimental studies, the investigation of complex RNA molecules through the detailed examination of individual structural motifs, and it is this property that is particularly suited to the approach described herein.

Experimentally, researchers have typically studied RNA stability by dissociating/unfolding RNA molecules. Traditionally, this has been done using heat to melt, or chemicals to denature the RNA. These methods are performed in relatively large volumes, require the averaging of data from considerable numbers of molecules, and are likely to involve a varied set of kinetic paths and transient states. Recently, however, single-molecule studies have begun to be employed to elucidate the complex processes of RNA folding. The single-molecule approach provides access to individual molecules within an ensemble, allowing further insights into the folding pathways. Fluorescence microscopy, for example, has provided information into the folding kinetics of individual ribozymes, and revealed a number of folding pathways, including some not previously observed by ensemble methods (Zhuang et al., 2000). Optical tweezers, meanwhile, have been employed to apply an external force to the ends of long RNA molecules causing them to ''unzip''. In these experiments, when the molecules were held at a critical force they were also shown to undergo rapid folding and refolding events, facilitating a study of such events under near equilibrium conditions (Liphardt et al., 2001, 2002). More recent investigations of the *T. thermophila* ribozyme have identified the location of kinetic barriers to mechanical unfolding (Onoa et al., 2003).

Atomic-force-microscopy-based force measurements have also been employed for the study of single nucleic acid molecules. Most of these studies have focused upon DNA, including investigations of the force-extension

Submitted April 3, 2003, and accepted for publication January 28, 2004.

Address reprint requests to Stephanie Allen, Laboratory of Biophysics and Surface Analysis, School of Pharmacy, University of Nottingham, University Park, Nottingham, UK NG7 2RD. Tel.: 44-0-115-9515050; Fax: +44-0-115-9515110; E-mail: stephanie.allen@nottingham.ac.uk.

0006-3495/04/06/3811/11 $2.00

doi: 10.1529/biophysj.103.026070

properties of DNA molecules of several hundreds to thousands of basepairs in length (Rief et al., 1999; Clausen-Schaumann et al., 2000), and the modification of such properties by various agents, including the binding of drugs (Krautbauer et al., 2002). In addition, various groups have demonstrated that it is possible to record interaction forces between individual complementary oligonucleotides, as force transducers (e.g., AFM probe) and surfaces functionalized with such molecules are brought into and out of contact (Noy et al., 1997; Strunz et al., 1999; Grange et al., 2001; Pope et al., 2001; Schumakovitch et al., 2002). In this type of experiment (termed dynamic force spectroscopy measurements if recorded over a range of loading rates; Evans and Ritchie, 1997, 1999; Evans, 1998, 2001; Merkel et al., 1999) a force is applied to the oligonucleotide complex formed during probe-sample contact, and the thermally induced dissociation event accelerated. Through this approach information upon energy barriers traversed during force-induced processes have been provided, and recent experiments have revealed how such data can be influenced by the length of the duplex probed (Strunz et al., 1999) and a change in the experimental environment (Schumakovitch et al., 2002). The following studies were performed to further extend this latter experimental approach through the investigation of the forced dissociation of a range of RNA oligonucleotides. For the analysis of RNA stability, this approach enables the modular nature of RNA to be exploited and provides a method to investigate the dissociation kinetics over located energetic barriers, and thus a means to explore the relative kinetic stabilities of small structural units.

The presented studies focus upon the forced dissociation of a 12-mer and 24-mer RNA double helix before and after the insertion of a putative trinucleotide bulge motif. The double helix itself is not considered a structural motif, because the length is arbitrary and the conformation remains unaltered by residue additions or deletions; however it is a dominant element within RNA molecules, accounting for as much as 50% of the residues in an average nonmessenger RNA molecule (Saenger, 1984). The structural diversity of RNA is provided by a combination of specific structural motifs inserted within these helical stretches. The bulge structure is one such motif, universally distributed through all structurally functional RNAs. It consists of a small number of unpaired residues in one strand, which may either extrude from the duplex or be accommodated by stacking between adjacent basepairs, and is known to play a biologically significant role within RNA molecules as it creates unique recognition sites within the RNA molecule.

The UCU bulge sequence studied in these experiments is found within a stretch of purine residues in the HIV-1 TAR (*trans*-activation response) element. This bulge has been the subject of comprehensive study, being the recognition site for the binding of the viral regulatory Tat protein (reviewed by Aboul-ela et al., 1996). Structural analysis of HIV-1 TAR has shown that the conformation of the molecule is influenced by the presence of magnesium ions (Zacharias and Hagerman, 1995; Ippolito and Steitz, 1998). Consequently, the dissociation of a duplex containing the UCU bulge structure was also studied in the presence and absence of magnesium ions to determine if changes in stability could be detected and characterized by dynamic force spectroscopy.

MATERIALS AND METHODS

All chemicals were obtained from Sigma Aldrich (Poole, UK) unless otherwise stated. Care was taken to eliminate ribonuclease contamination from the experiment by employing sterile techniques in the preparation of samples. In addition, gloves were worn at all times and sterilized, disposable plasticware was used where possible. All water used was of 18 MΩ cm resistivity and was pretreated overnight with diethylpyrocarbonate (DEPC, 0.05% v/v) before being autoclaved for 30 min. All solutions were passed through sterile 0.2 μm Minisart filters (Sartorius AG, Göttingen, Germany) before use, all work surfaces including the AFM liquid cells were wiped with an RNase inhibitor (RNaseZap), and the liquid cell was rinsed thoroughly before use.

Functionalization of AFM surfaces

Short RNA oligonucleotides were synthesized with a ''Phosphoramidite 18'' linker (Oswell Research Products, University of Southampton, UK), with a hexaethyleneglycol phosphoramidite-thiophosphate linker at the 5′ terminus resulting in a free thiol at the 5′ end of the molecule. The free thiol functionality was included to facilitate covalent attachment to gold surfaces and AFM probes, and the ethyleneglycol linker molecules to space the oligonucleotide away from the underlying substrate and thus minimize its impact upon the interaction (Hinterdorfer et al., 2000). Gold-coated surfaces (Hegner et al., 1993) and AFM probes were then functionalized with these oligonucleotides to produce the self-assembled monolayer architecture described by Noy et al. (1997). Undecanol-thiol was incorporated into the incubation mixture at 200-fold higher concentration to dilute the RNA surface density and ensure a high probability for the formation of single RNA duplexes.

To prepare the interacting surfaces, AFM cantilever probes (NanoProbes, Veeco, Santa Barbara, CA; nominal spring constants 10–55 pN/nm), which had been gold sputter-coated, and template-stripped gold substrates were incubated overnight at room temperature in 1 μM oligonucleotide solutions, 200 μM undecanol-thiol, 75% (v/v) ethanol, 40 mM Tris buffer, pH 7. The surfaces were then rinsed in 20 mM Tris buffer, pH 7, 10 mM $MgCl_2$ for use in force-spectroscopy experiments the same day. $MgCl_2$ was omitted from the wash for experiments performed in the absence of magnesium ions.

Four distinct duplexes were studied in the course of these experiments (Table 1). The first required the tip to be functionalized with the 12-mer sequence GCGUUUUUUGCG while the substrate was coated with its fully complementary sequence. For the second series of experiments, the same 12-mer bulge duplex sequence was used on the tip and a 15-mer oligonucleotide, based on the complementary sequence with a UCU trinucleotide incorporated at positions 7–9, on the substrate. The third duplex consisted of a 24-mer fully complementary sequence related to the 12-mer sequence, but with an extended run of adenine-uracil basepairs. The fourth experimental configuration aimed to investigate the impact of the UCU trinucleotide bulge (inserted at positions 13–15) upon the forced dissociation of the 24-mer duplex. Again these experiments employed tips functionalized with a 24-base oligomer, while the substrates were coated with the complementary sequence containing the trinucleotide bulge sequence.

The dodecamer sequence was chosen to promote the formation of a single 12-mer duplex, to avoid collecting data from a number of duplexes formed

TABLE 1 The duplex sequences studied by dynamic force spectroscopy

Name	Duplex sequence
12-mer	CGCAAAAAACGC GCGUUUUUUGCG
12-merB	UCU CGCAAA AAACGC GCGUUU---UUUGCG
24-mer	CGCAAAAAAAAAAAAAAAAAACGC GCGUUUUUUUUUUUUUUUUUGCG
24-merB	UCU CGCAAAAAAAAA AAAAAAAAACGC GCGUUUUUUUUU---UUUUUUUUUGCG

by partially overlapping strands. Examination of this sequence reveals that the maximum number of interacting complementary basepairs within a partial overlap is six, and it is anticipated that formation of this structure is significantly less favorable than the fully complementary 12 mer. A similar lack of partial overlapping is expected from the 12-mer bulge-containing sequences. 24-mer sequences were chosen as to provide extended structures with sequences related as closely as possible to that of the 12-mer and 12-mer bulge sequences. Importantly, in none of the putative duplexes could the UCU bulge nucleotides form complementary basepairs with the opposing strand.

Force-distance experiments

Force-distance measurements were carried out using the Molecular Force Probe (Asylum Research, Santa Barbara, CA). In most instances, experiments were performed in 20 mM Tris, pH 7, 10 mM $MgCl_2$. The exception to this was when studying the effect of the absence of magnesium ions, when the $MgCl_2$ was omitted. In all cases an RNA-functionalized tip at the end of a flexible cantilever was brought into and out of contact with an RNA-modified surface. The gradient of the retract trace when the tip was in contact with a hard surface enabled the measured detector signal to be converted into actual deflection (Lee et al., 1994), allowing the horizontal distance axis to be corrected from *z*-piezo displacement to tip-sample separation. The force of interaction between tip and sample was then determined by Hooke's law, as a product of the cantilever spring constant and the cantilever deflection distance. The spring constant of each cantilever used was ascertained through thermal fluctuations of the cantilever (Hutter and Bechhoefer, 1993).

Applied loading rates were approximated as the product of the cantilever spring constant and the piezo retract velocity (Evans, 1998), as our measurements were dominated by cantilever loading. This approximation was made because the linker molecules employed in our studies were short (~2–3 nm per RNA molecule) and the cantilevers used were soft. Both velocity and cantilever spring constant were varied during the course of the study to provide the required range of rates. At least 800 force curves were collected at each loading rate and the specificity of the tip-substrate interaction confirmed by blocking the substrate with an excess of the complementary sequence.

RESULTS

Analysis of force-distance data

Only force-distance curves attributed to specific interactions between RNA molecules were analyzed within our experiments. It should be noted that control experiments confirmed that specific interactions did not occur between surfaces functionalized only with undecanol-thiol spacer molecules, whereas previous experiments have shown that specific interactions are not observed when surfaces are functionalized with identical oligonucleotides (Pope et al., 2001). As seen in Fig. 1, it was possible to separate specific interaction events from the small number of curves showing nonspecific interactions due to a change in the gradient of the retract slope observed in force-distance curves derived from specific interactions (Willemsen et al., 1998). This arose because the specific interactions occurred with rupture lengths

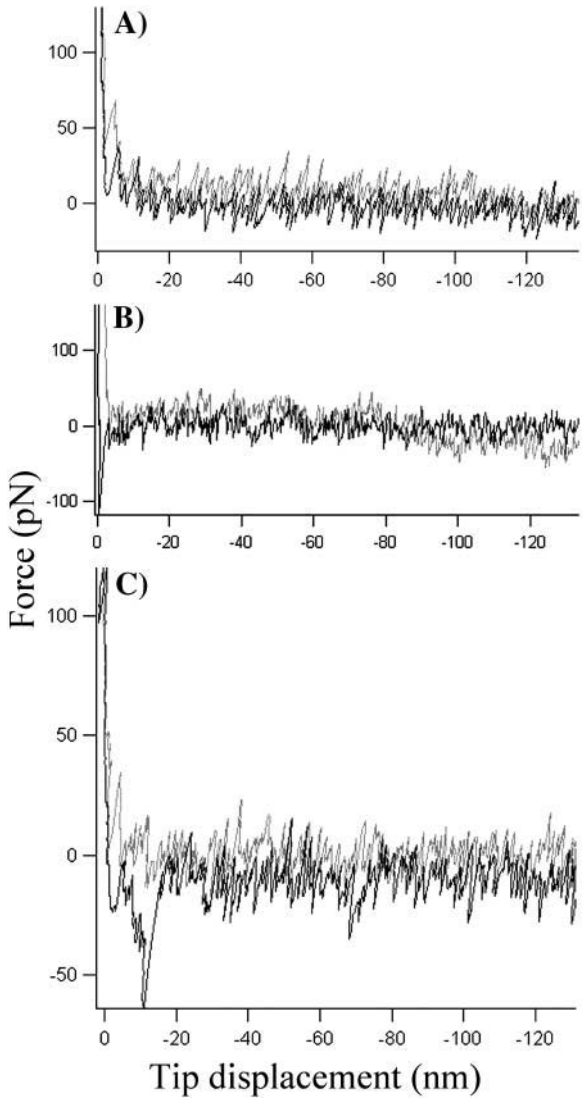

FIGURE 1 Examples of the types of force curves observed between RNA functionalized AFM surfaces and tips; each curve has been corrected to show force against tip-sample displacement. In each example the approach trace is shown in gray and the retract trace in black. (*A*) No interaction has occurred between the tip and substrate. (*B*) A nonspecific interaction between the two surfaces, with no observable change in the gradient of the retraction slope. (*C*) A specific interaction between the two RNA functionalized surfaces, showing a stretch of ~10 nm before the rupture event.

approximately equivalent to the length of the RNA molecule plus twice the length of the linker, whereas nonspecific adhesions occurred with a rupture length of zero. The combined length of two fully extended hexaethyleneglycol linkers is ~4 nm (assuming a length of ~3.4 Å per ethytleneglycol monomer), and neglecting the geometry of the tip/sample contact a 12-mer RNA duplex before extension would be ~3.4 nm and a 24-mer RNA duplex ~6.8 nm. Little variation in the mean rupture length was actually observed between all the experiments and a mean rupture length of 11.5 ± 7.6 nm was calculated for all the force curves analyzed.

In each experiment, the proportion of force curves that resulted in a specific interaction between the two surfaces was determined. If they arose more frequently than one force-distance curve in five the experiment was discarded because the probability that multiple interactions were occurring became too high (Williams and Evans, 2001). In the presented study from between one in five and one in 12 of the curves demonstrated a specific interaction. At the end of the experiment, to verify the specificity of the probe-sample interaction, the surface was incubated with the complementary RNA molecule, reducing further the number of specific sites available for interaction with the functionalized tip. After this blocking stage the frequency of force curves showing a specific interaction fell by a minimum of 50%, confirming that the observed interactions were between complementary RNA strands.

Histograms were plotted of the obtained specific dissociation forces at each of the loading rates employed. Examples of the histogram plots obtained for the four duplexes at a range of loading rates are shown in Figs. 2 and 3. For each experiment the peak dissociation force was then plotted as a function of the logarithm of the loading rate to provide dynamic force spectra (Figs. 2 and 3), and values for the zero-force dissociation rate (k_{off}) and the thermal force scale (f_β) determined as previously described (Evans, 1998, 2001; Merkel et al., 1999; Evans and Ritchie, 1999).

It should be noted that each symbol within the presented dynamic force spectra indicates a peak dissociation force that was obtained from interactions using one cantilever and substrate. If a symbol is repeated within one plot it signifies that the data point was obtained by altering the retract velocity of the cantilever. It can be seen from this that dissociation forces obtained both from the same cantilever at varying velocities and from different cantilevers show the same response to a change in loading rate. In accordance with the theoretical description of bond dissociation under applied force, a linear increase in the peak dissociation force with a logarithmic increase in loading rate was observed in all cases. This indicates that, in our experiments, duplex

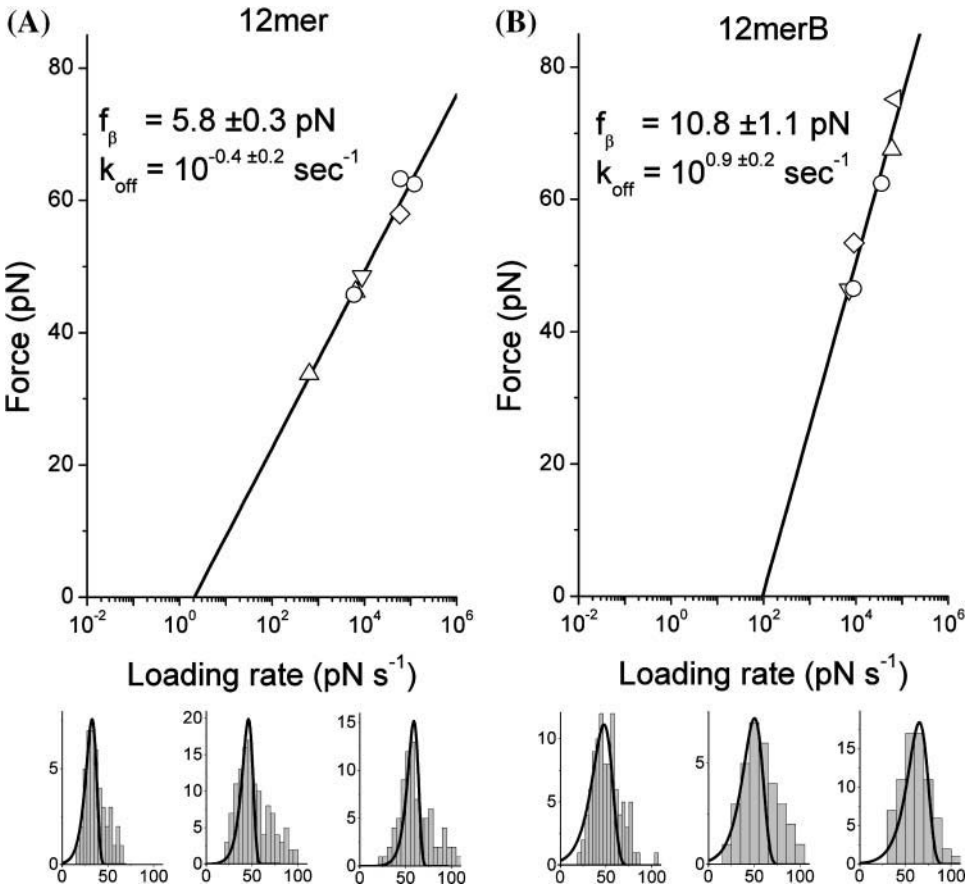

FIGURE 2 Dynamic force spectra for (*A*) the 12-mer and (*B*) 12-mer B experiments. Also displayed are examples of histograms for each experiment showing the distribution of dissociation forces obtained at a range of loading rates; namely 646 (*left*), 6460 (*middle*), and 60,290 (*right*) pN s^{-1} for the 12-mer and 7048 (*left*), 8906 (*middle*), and 35,891 (*right*) pN s^{-1} for the 12-mer B experiments, respectively.

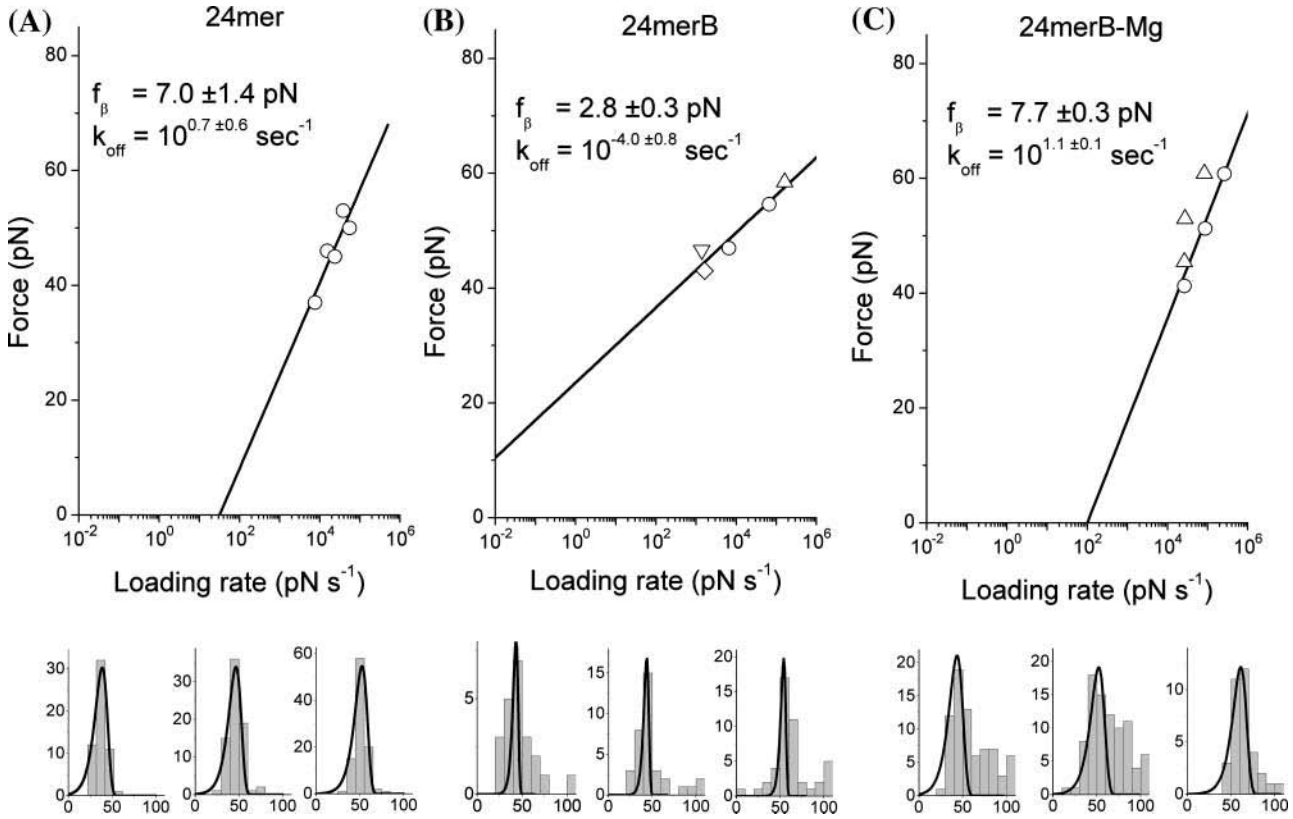

FIGURE 3 Dynamic force spectra for the (*A*) 24-mer, (*B*) 24-mer B, and (C) 24-mer B-Mg experiments. Example histograms for each experiment showing the distribution of dissociation forces at a range of loading rates are also displayed; namely 7691 (*left*), 23,886 (*middle*), and 55,734 (*right*) pN s^{-1} for the 24-mer; 1391 (*left*), 1653 (*middle*), and 66,290 (*right*) pN s^{-1} for the 24-mer B; and 27,632 (*left*), 83,480 (*middle*), and 264,300 (*right*) pN s^{-1} for the 24-mer B-Mg experiments, respectively.

separation occurred within the thermally active regime and that a single energy barrier was being probed in each experiment (Evans and Ritchie, 1997), albeit over the very narrow range of rates possible with the AFM.

Values for k_{off} and f_β (Table 2) were derived from each dynamic force spectrum by least squares fitting through the points, and these data used to predict the full distribution of dissociation forces at the rates tested (Evans and Williams, 2001). Superimposed upon each data histogram is that predicted for correlated bond failure, assuming no experimental error. It can be seen that, particularly at the lower range of dissociation forces, there is good agreement between this model distribution and the experimental data; however, at higher forces more frequent events are sometimes observed in the experimental data than are predicted by the model. We attribute these higher force interactions to the low frequency incidence of multiple RNA interactions between the tip and substrate. Finally, ranges for the estimated k_{off} and f_β values (Table 2) were determined by applying the ''bootstrap'' Monte Carlo resampling method (Press et al., 1992) with 100 replacements to the peak dissociation forces obtained at the varying loading rates.

TABLE 2 The dissociation rate (k_{off}) and force scale (f_β) determined for all the duplexes studied

Name	k_{off} (s^{-1})	f_β (pN)	Approximate k_{off}/k_{off} (12-mer)	Approximate f_β/f_β (12-mer)
12-mer	$10^{-0.4 \pm 0.2}$	5.8 ± 0.3	1	1
12-merB	$10^{0.9 \pm 0.2}$	10.8 ± 1.1	20	2
24-mer	$10^{0.7 \pm 0.6}$	7.0 ± 1.4	13	1.2
24-merB	$10^{-4.0 \pm 0.8}$	2.8 ± 0.3	0.0003	0.5
24-merB-Mg*	$10^{1.1 \pm 0.1}$	7.7 ± 0.3	32	0.8

Approximate factors, relative to the 12-mer data, for k_{off} and f_β are also provided.

*Experiment performed in the absence of Mg^{2+}.

Although there are several potential sources of error within these measurements, the error associated with calibration of the cantilever spring is likely have the most impact, with an absolute uncertainty estimated at ~10% (Florin et al., 1995). The influence of this uncertainty is, however, reduced in our experiments because data sets were obtained using both a number of different cantilevers and a range of retract velocities for the same cantilever, and in all instances the experimentally obtained peak dissociation force demonstrated a comparable linear response to the logarithm of the loading rate. It should also be noted that the good agreement

between data obtained with different cantilevers, and their response to loading rate, is further evidence that our measurements are dominated by cantilever loading.

Dissociation of a 12-mer fully complementary duplex

Experiments were first performed using the two 12-mer fully complementary RNA strands (Table 1). Peak dissociation forces between 34 and 61 pN were observed with the range of loading rates employed (646–120 580 pN s^{-1}), a k_{off} value of $10^{-0.4\pm0.2}$ s^{-1} was estimated for the complementary RNA dodecamer duplex. This value lies in the range of $10^{-0.7}$–$10^{0.2}$ s^{-1} published for a DNA duplex of the analogous sequence (Pope et al., 2001). Meanwhile, the f_β of 5.8 ± 0.3 pN determined for the dissociation of the RNA duplex indicates that the energy barrier to the dissociation of the short RNA duplex was situated ~0.7 nm along the reaction coordinate (given $f_\beta = k_BT/x_\beta$, where x_β is the projected distance along the dissociation reaction coordinate to the transition state (Evans, 1998, 2001; Merkel et al., 1999; Evans and Ritchie, 1999).

Dissociation of a 12-mer duplex containing a trinucleotide bulge sequence

When the UCU trinucleotide sequence was inserted into positions 7–9 of the purine-rich strand of the 12-mer RNA duplex (hereon referred to as 12-merB), forming a putative bulge structure (Table 1), peak dissociation forces between 59 and 81 pN were observed for the range of loading rates employed (7048–71 400 pN s^{-1}). The presence of this bulge motif caused an almost twofold increase in f_β from 5.8 ± 0.3 pN to 10.8 ± 1.1 pN. This increase was also reflected in a broader distribution of dissociation forces at each loading rate. This doubling in force scale reflects a halving of the projected distance to the probed barrier. A 20-fold increase in the observed k_{off} to $10^{0.9\pm0.2}$ s^{-1} was also observed.

Dissociation of a 24-mer fully complementary duplex

To investigate the influence of duplex length, experiments were also performed with a fully complementary 24-mer sequence (see Table 1). Peak dissociation forces between 37 and 53 pN were observed with the range of loading rates employed (7691–38 460 pN s^{-1}), revealing an f_β of 7.0 ± 1.4 pN and a k_{off} value of $10^{0.7\pm0.6}$ s^{-1}.

Dissociation of a 24-mer duplex containing a trinucleotide bulge sequence

The impact of the same bulge sequence upon the 24-mer dissociation was also investigated. In these experiments the UCU bulge was inserted at positions 13–15 in the purine-rich strand (Table 1). This 24-mer bulge duplex (24-mer B) produced peak dissociation forces between 47 and 59 pN at the loading rates utilized (1391–161 800 pN s^{-1}). The 24-mer B data provided a force scale of 2.8 ± 0.3 pN and a dissociation rate of $10^{-4.0\pm0.8}$ s^{-1}.

Effects of magnesium on the stability of a bulge duplex

The experiments performed upon the 24-mer bulge duplex oligonucleotides were also performed in the absence of $MgCl_2$ (24-mer B-Mg), to investigate the sensitivity of the measurement to the presence of Mg^{2+} ions. Peak dissociation forces in the range 44–61 pN were observed for loading rates between 26,430 and 264,300 pN s^{-1}. The force scale determined (7.7 ± 0.3 pN) is greater than that observed in the presence of magnesium ions and there is a 10^5-fold increase in the estimated dissociation rate ($10^{1.1\pm0.1}$ s^{-1}) of the 24-mer bulge duplex without magnesium ions, indicating a considerable decrease in kinetic stability.

DISCUSSION

Analysis of RNA dissociation: dissociation of a fully complementary 12-mer duplex

This research shows the first application of dynamic force spectroscopy for probing the dissociation pathways of short RNA duplexes. It is of note that a comparison of the dissociation rate determined in this study for the RNA 12-mer with that published for the analogous DNA 12-mer indicates a comparable kinetic stability (Pope et al., 2001), although it is generally considered that an RNA molecule is much more stable than its DNA equivalent (Freier et al., 1986). It has, however, been shown that both A_n and A_nT_n sequences stabilize DNA through the formation of an alternate B′ structure that possess three-centered hydrogen bonds within the A-tract (Mukerji and Williams, 2002); furthermore, studies suggest that an analogous sequence within RNA substantially destabilizes the duplex. As a result an RNA duplex containing these sequences, such as the 12-mer in this study, would indeed be expected to have a similar thermodynamic stability to its analogous DNA duplex (Conte et al., 1997).

A force scale of 5.8 ± 0.3 pN was determined for the short 12-mer RNA duplex, indicating that the energy barrier to dissociation was situated 0.7 nm (i.e., ~0.06 nm per basepair) from a ground state. However, for the analogous DNA sequence, a force scale of 7 pN has been published (Pope et al., 2001) indicating that the barrier displacement is slightly smaller for DNA (~0.05 nm per basepair). The reason for this has not been clearly identified; however, it is interesting to note that an RNA duplex exists in the A-helical form, with an axial rise of 0.28 nm per basepair, whereas a DNA duplex usually exists in a B-form with a greater axial

rise of 0.34 nm per basepair (Saenger, 1984). It could be postulated that a proportionally greater extension is required for the dissociation of the more compact RNA duplex. In this way the ~1.2-fold difference in x_β between the two oligonucleotides may be a consequence of the ~1.2-fold difference in the axial rise.

Previous research (Strunz et al., 1999; Grange et al., 2001) has demonstrated that during the force-induced dissociation of short DNA duplexes (between 10 and 30 basepairs in length), the distance along the energy landscape from the bound state to the energy barrier to dissociation increases linearly with the number of basepairs, while the dissociation rate decreases exponentially with basepair number. This exponential response can be attributed to the energy required for dissociation increasing linearly with basepair number (Strunz et al., 1999), and indicates that short DNA duplexes respond cooperatively to a force when loads are applied to the 5′ termini of opposing strands. Due to the similarities in the apparent force-induced behaviors of RNA and DNA, and also between the employed experimental methodology and those previously reported for DNA, from hereon it was assumed that RNA oligonucleotides must also undergo similar cooperative dissociation events upon the application of force.

Dissociation of a 12-mer duplex containing a bulge motif

Inclusion of a trinucleotide bulge motif within the 12-mer duplex (to provide the 12-mer B duplex), was found to result in a doubling of the force scale and a 20-fold increase in the extrapolated dissociation rate. For cooperative bond failure this affect on the force scale could arise if the length of the duplex formed was reduced to six basepairs. However, as we show later the 20-fold increase in observed k_{off} to $10^{0.9\pm0.2}$ s^{-1} is much less than expected if only a 6-mer duplex was broken through a cooperative rupture process, and suggests that a bulge-containing structure is being created. Introducing an angle, θ_F, between the reaction coordinate and the applied force could also account for a change in the force scale by $1/\cos(\theta_F)$ (Evans, 1998). Previous research has shown that the HIV-1 TAR molecule displays a bend at the point of the UCU bulge motif (Zacharias and Hagerman, 1995); however, this bend has been shown to be only ~25° and as such would result in a minimal change in the projection of force and is thus not sufficient to account for the observed effects.

There are two possible explanations for the observed effects of the bulge motif upon duplex stability. Firstly, the insertion of the bulge into a complementary duplex could be breaking the cooperativity of dissociation, resulting in the formation of three independent components, i.e., two shorter helices and the bulge itself. Alternatively, the cooperativity may be being maintained and the complexity of the dissociation landscape increased. If the cooperativity had been disrupted through the insertion of the bulge, the lifetime of the interaction for the complete system would be equivalent to the sum of the lifetimes of the three individual components. In this scenario, the impact of a given bulge sequence would be constant and independent of the lengths of surrounding helices; the combined lifetime of the two shorter helixes on either side of the bulge motif would be ~1.5-fold greater than the lifetime of a single duplex of the same length, because it is assumed that there would be an equal probability of either helix failing first. Thus, the interaction lifetime for a 24-mer duplex containing a UCU bulge motif would be the sum of the lifetime of the UCU bulge and 1.5 times the lifetime of the 12-mer duplex, i.e.,

$$1/k_{\text{off24merB}} \approx 1/k_{\text{offBulge}} + 1/k_{\text{off12mer}} + 1/2k_{\text{off12mer}}.$$

Consideration of the data obtained from the 12-mer duplex indicates that the combined lifetime of the two 12-mer halves within the 24-mer B bulge-containing duplex would be short ($k_{off} \sim 10^{-0.6} s^{-1}$) compared to the total lifetime of the 24-mer B complex ($k_{off} = 10^{-4.0}$ s^{-1}). This in turn suggests that the bulge would be the dominant contributor to stability ($k_{off} \sim 10^{-4.0}$ s^{-1}). Because in this scenario, the lifetime of the bulge should be independent of the lengths of the surrounding helices, the stability of this bulge within the 24-mer B duplex would be the same within the 12-mer B duplex. However, it can be seen that the dissociation rate for the complete 12-mer B duplex containing the same UCU trinucleotide bulge ($k_{off} = 10^{0.9}$ s^{-1}) is significantly faster than the presumed lifetime of this bulge component. This demonstrates that the lifetime of a complete bulge-containing duplex is not simply a sum of its components. Hence, this indicates that there is no disruption to the cooperativity of unbinding after insertion of the bulge motif; rather there is an increase in the complexity of the dissociation landscape.

A comparison of the location of the energy barrier for the 12-mer and 12-mer B duplexes provides further information regarding the dissociation landscape after the insertion of the bulge. It can be seen that in the 12-mer B data, alongside an increase in the complexity of the landscape, there is also a doubling in the force scale. This change in barrier displacement without an accompanying change in basepair number reveals that the 12-mer B experiments must be probing an additional barrier introduced with the insertion of the bulge. The presence of this additional barrier after the insertion of the bulge indicates that an unstable intermediate structure must exist between the fully bound and unbound states. It can also be seen that the location of this additional transition state along the dissociation coordinate can be related to the cooperative response from half the number of basepairs within the duplex and thus may be associated with the location of the bulge motif within the duplex, although this relationship needs to be confirmed by further experimentation.

Dissociation of a fully complementary 24-mer duplex

The experiments performed with the fully complementary 24-mer duplex revealed a force scale of ~7 pN, and a dissociation rate of $10^{0.7\pm0.6}$ s^{-1}. These results, however, differ markedly from those expected. Indeed, from our 12-mer data, we expect a 24-mer duplex to provide a force scale of ~2.9 pN. The results thus indicate that either the force-induced dissociation of RNA oligonucleotides is not a cooperative process or that only a partial duplex, equivalent to 10 basepairs, was formed and broken during our measurements. However, there is no indication in the literature that cooperative bond rupture should not occur in RNA molecules, and thus we felt that the latter scenario was more likely. Therefore to investigate this phenomenon further, and to complete our series of experiments, we continued our studies to investigate the forced dissociation of a 24-mer duplex containing a bulge motif.

Dissociation of a 24-mer duplex containing a bulge motif

Within these experiments the dissociation rate for the 24-mer B duplex was determined to be less than that for the fully aligned 12-mer duplex, confirming that a more stable, and hence longer duplex had been formed. The force scale obtained is also less than that obtained for the 12-mer B bulge-containing duplex, indicating either an increase in the displacement of the energy barrier or a change in the transition state being measured. Interestingly, however, the force scale is more reflective of that expected for a fully aligned 24-mer duplex, it being approximately half of the value determined for the 12-mer duplex.

Comparison of the data from the two bulge-containing duplexes reveals that, whereas in the 12-mer B experiments an intermediate transition state attributed to the presence of the bulge was being probed, in the 24-mer B duplex experiments a transition state more reflective of the fully aligned duplex was dominant. The observed halving of the force scale apparent through comparison of the 24-mer B with the 12-mer data also suggests that the 24-mer B is following a similar dissociation process.

The failure to detect this duplex-related barrier in the 12-mer B experiments, with a force scale of 6 pN of the 12-mer, arises because the required loading rates are lower than those currently accessible via the AFM. However, the inability to detect the intermediate barrier introduced by the bulge in the 24-mer B experiments must indicate that this barrier does not scale with duplex length, and is due therefore to the properties of the bulge and not the duplex.

Comparison of 24-mer and 24-mer B data also reveals a discrepancy in the apparent number of basepairs being probed in these experiments. Indeed the data indicate that for the 24-mer experiments only 10 basepairs are able to form, whereas in the 24-mer B experiments, the presence of bulge appears to help all 24 complementary basepairs form. Although this is difficult to explain, we note that oligonucleotides containing poly(A) tracts are known to be curved (Ulanovsky and Trifonov, 1987). We postulate that for our 24-mer sequence, this property may hinder the formation of the fully complementary duplex in these experiments. In contrast, a change in flexibility provided through inclusion of trinucleotide bulge into the sequence may help the sequence to fully align.

The effect of magnesium on bulge stability

To investigate the sensitivity of our measurement to the presence of Mg^{2+} ions, measurements were also recorded for the 24-mer B, in the absence of $MgCl_2$ (termed 24-mer B-Mg experiments from hereon). From the obtained force scales and dissociation rates, both the displacement of the energy barrier and the stability of the 24-mer B-Mg duplex are less than those found for the fully complementary 12-mer. The 24-mer B-Mg data are much closer to those obtained for the 24-mer sequence (without bulge), suggesting that in these experiments a shorter duplex resulting through a partial interaction of the two RNA strands is also being probed, and supports our hypothesis that the bulge aids the full duplex formation of the long poly(A) tract. Using the distance of 0.06 nm per basepair value determined from the 12-mer duplex, the 24-mer B-Mg data is in fact more indicative of the rupture of a nine-basepair duplex.

These data thus suggest that the presence of magnesium ions helps to stabilize the RNA duplex containing the UCU trinucleotide bulge structure. This is in agreement with the literature that states that RNA can be stabilized by the presence of magnesium ions in specific binding pockets within an RNA molecule (Pörschke, 1977; Serra et al., 2002). Such a binding pocket has been identified within the UCU motif in the HIV-1 TAR element. The extruded bulge within the TAR element has been shown to be stabilized by three divalent cations, which through coordination to the phosphate groups allow for a sharp turn in the RNA backbone (Zacharias and Hagerman, 1995) enabling the opposing strand to remain in a conformation close to the A-form (Ippolito and Steitz, 1998). Meanwhile, in the absence of divalent cations, the unpaired bases of the bulge point inside the duplex, stacking onto residues of the flanking stems that are themselves kinked relative to each other (Aboul-ela et al., 1996), distorting and destabilizing the duplex. As a result, the bend angle at the point of the UCU motif in the HIV-1 TAR element increases twofold in the absence of these divalent cations (Zacharias and Hagerman, 1995).

Estimating transition state energies and kinetic prefactors

The dissociation rates for the 12-mer and the partially formed duplexes, the 24-mer, and 24-mer B without magnesium

(24-mer B-Mg), permit an estimation of the average contribution of each basepair to the transition state energy, alongside the corresponding estimation of the exponential prefactor of the dissociation kinetics. Under cooperative failure the duplex can be considered as the compound bond and, neglecting any sequence dependence, a generic expression for the dissociation rate can be written as

$$k_{\mathrm{off}}(N) \approx \frac{1}{N\tau_{\mathrm{D}}}\exp\left(-\frac{N\overline{E_{\mathrm{b}}}}{k_{\mathrm{B}}T}\right), \qquad (1)$$

with each basepair adding E_{b} of energy to the transition state; where N is the number of basepairs (where $N = (k_{\mathrm{B}}T / f_{\beta})/(x_{\beta}$ per basepair, as determined from our 12-mer data), or $\sim 70 / f_{\beta}$) and τ_{D} is the diffusional relaxation time. Using

$$\log_{\mathrm{e}}[Nk_{\mathrm{off}}(N)] = -\frac{\overline{E_{\mathrm{b}}}}{k_{\mathrm{B}}T}N + \log_{\mathrm{e}}\left(\frac{1}{\tau_{\mathrm{D}}}\right), \qquad (2)$$

Fig. 4 shows the estimation of E_{b} and $1/\tau_{\mathrm{D}}$ of 1.1 k_{B}T/b.p. and 2×10^{6} s^{-1}, respectively. We are, of course, wary of the considerable variance in these estimates. The 1.1 k_{B}T/b.p. contribution to the transition state energy may also at first seem unreasonably low as it is similar to estimates of the thermodynamic stability per basepair. However, under force the molecule is likely to undergo some conformational change (stretch) before dissociation and so here we are not measuring the transition state energy relative to the ground state but rather from a destabilized form (Pope et al., 2001). We reiterate, therefore, that our measurements and predictions of rate above are for dissociation under force. The kinetic prefactor suggests a diffusional relaxation time of a few hundred nanoseconds, and lying between the nanoseconds for the diffusion of small ligands and the microseconds of proteins (Schuler et al., 2002), it also seems a reasonable estimate. It should be noted that this relaxation time is comparable to the longest timescale currently available for atomistic molecular simulation.

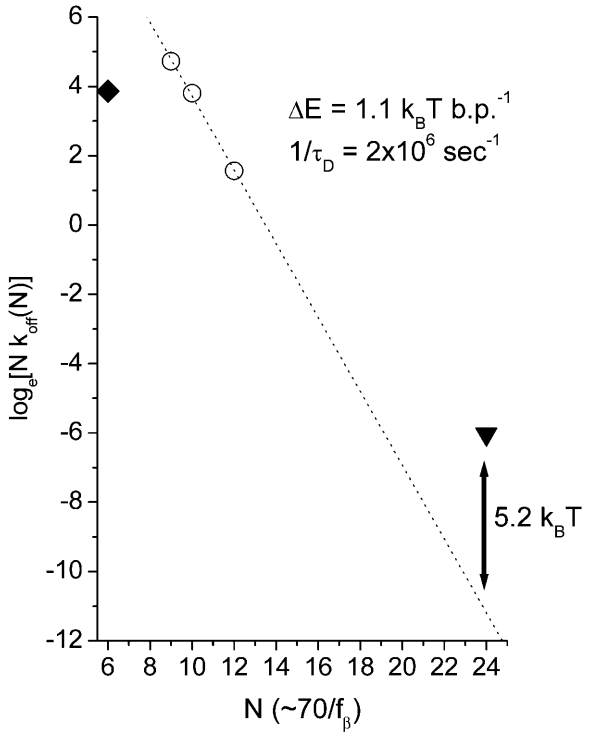

FIGURE 4 Using Eq. 2, a plot of $\log_{\mathrm{e}}[Nk_{\mathrm{off}}(N)]$ versus N reveals estimates for the contribution of each basepair to the probed transition states (ΔE), and also the exponential prefactor for dissociation kinetics ($1/\tau_{\mathrm{D}}$).

Plotted also in Fig. 4 are the data for the 12-mer B (*diamond*) and 24-mer B with magnesium (*triangle*). Although the data for the sequences in which only simple duplexes are formed (i.e., the 12-mer, 24-mer, and 24-mer Mg data) lie on the same line, the 12-mer B dissociation profile differs significantly, supporting our conclusion that the transition state measured in this dissociation is of a bulge formed in a 12-mer duplex and not dissociation of a partially formed 6-mer. Using the values of E_{b} and $1/\tau_{D}$ Eq. 1 permits us to estimate how a 6-mer duplex would behave under force and contrast this to that of the 12-mer B. The dissociation rate of a 6-mer duplex is calculated to be ~ 450 s^{-1}, which is 60 times faster than we measured for the 12-merB. With a force scale of ~ 12 pN, a 6-mer would require loading at $>30{,}000$ pN s^{-1} to measure a force above 20 pN, and such a study would therefore require the use of cantilevers with much greater stiffness and consequently different immobilization chemistries. The dissociation rate of the 12-mer B, therefore, cannot be compared to the other duplexes as the transition state being measured is clearly different.

In addition, the 24-mer B (in the presence of Mg^{2+}) dissociates at a rate significantly faster than we extrapolate for a 24-mer. The increase in rate is equivalent to a reduction in the energy to dissociate of around 5 k_{B}T. Nearest-neighbor predictions (Mathews et al., 1999) have suggested that upon insertion of a UCU bulge there is a drop in stability of ~ 7 k_{B}T (with the inclusion of terminal AU penalty terms; Xia et al., 1998), suggesting the duplex is only partly structured in the transition state, if at all. This again is consistent with the presence of a bulge-induced transition state on the dissociation landscape, which is crossed before the final dissociation event.

CONCLUSIONS

The presented study has revealed single-molecule dissociation data for RNA molecules of increasing structural complexity. We have demonstrated that a simple RNA duplex dissociates in a comparable manner to that previously reported for DNA duplexes of similar length. With this behavior in mind, we were able to show that the incorporation of a bulge motif adds complexity to the force-induced dissociation landscape through the introduction of an additional barrier. Interestingly, there has been some

published evidence for the existence of an intermediate in the dissociation pathway of a bulge-containing structure in solution experiments (Davis et al., 1998). Most significantly, studies have demonstrated that many bulge-containing RNA species do not melt in a two-state manner (Longfellow et al., 1990).

The destabilizing effect by a bulge motif has been observed in a number of solution melting studies (Longfellow et al., 1990; Leblanc and Morden, 1991; Zagórowska and Adamiak, 1996). Through experiments performed with longer 24-mer oligonucleotides we were able to estimate the destabilizing effect of the introduced UCU bulge motif, and also demonstrate its sensitivity to the presence of magnesium ions. Importantly, through consideration of all of the presented data we could also provide estimates for the contribution of each basepair to the explored transition states, and for the exponential prefactor for dissociation kinetics.

Our results thus demonstrate the potential of single-molecule dynamic force measurements to profile the dissociation landscapes of RNA molecules and to also probe the impact of specific motifs upon their kinetic stabilities. We believe that such experiments, together with the other single-molecule approaches currently under development, promise to profoundly impact upon our understanding of RNA stability and dissociation energetics.

Thanks go to Kelvin Chung for his help in obtaining the results in the absence of magnesium ions.

N.H.G. thanks the BBSRC for funding and S.A. thanks Pfizer Global Research and Development for funding her lectureship. P.M.W. is an EPSRC Advanced Research Fellow.

REFERENCES

Aboul-ela, F., J. Karn, and G. Varani. 1996. Structure of HIV-1 TAR RNA in the absence of ligands reveals a novel conformation of the trinucleotide bulge. *Nucleic Acids Res.* 24:3974–3981.

Brion, P., and E. Westhof. 1997. Hierarchy and dynamics of RNA folding. *Annu. Rev. Biophys. Biomol. Struct.* 26:113–137.

Clausen-Schaumann, H., M. Rief, C. Tolksdorf, and H. E. Gaub. 2000. Mechanical stability of single DNA molecules. *Biophys. J.* 78:1997–2007.

Conte, M. R., G. L. Conn, T. Brown, and A. L. Lane. 1997. Conformational properties and thermodynamics of the RNA duplex r(CGCAAAUUUGCG)$_2$: comparison with the DNA analogue d(CGCAAATTTGCG)$_2$. *Nucleic Acids Res.* 25:2627–2634.

Davis, T. M., L. McFail-Isom, E. Keane, and L. D. Williams. 1998. Melting of a DNA hairpin without hyperchromism. *Biochemistry.* 37:6975–6978.

Evans, E. 1998. Energy landscapes of biomolecular adhesion and receptor anchoring explored with dynamic force spectroscopy. *Faraday Discuss. Chem. Soc.* 111:1–16.

Evans, E. 2001. Probing the relationship between force—lifetime—and chemistry in single molecular bonds. *Annu. Rev. Biophys. Biomol. Struct.* 30:105–128.

Evans, E., and K. Ritchie. 1997. Dynamic strength of molecular adhesion bonds. *Biophys. J.* 72:1541–1555.

Evans, E., and K. Ritchie. 1999. Strength of a weak bond connecting flexible polymer chains. *Biophys. J.* 76:2439–2447.

Evans, E., and P. Williams. 2001. Dynamic force spectroscopy. I. Single bonds. *In* Les Houches Session LXXV Physics of Bio-Molecules and Cells. H. Flyvbjerg, F. Jülicher, P. Ormos, and F. David, editors. Springer-Verlag, Berlin, Germany. 145–186.

Florin, E. L., M. Rief, H. Lehmann, M. Ludwig, C. Dornmair, V. T. Moy, and H. E. Gaub. 1995. Sensing specific molecular-interactions with the atomic-force microscope. *Biosens. Bioelectron.* 10:895–901.

Freier, S. M., R. Kierzek, J. A. Jaeger, N. Sugimoto, M. H. Caruthers, T. Neilson, and D. H. Turner. 1986. Improved free-energy parameters for predictions of RNA duplex stability. *Proc. Natl. Acad. Sci. USA.* 83:9373–9377.

Grange, W., T. Strunz, I. Schumakovitch, H.-J. Güntherodt, and M. Hegner. 2001. Molecular recognition and adhesion of individual DNA strands studied by dynamic force spectroscopy. *Single Mol.* 2:75–78.

Hegner, M., P. Wagner, and G. Semenza. 1993. Ultralarge atomically flat template-stripped Au surfaces for scanning probe microscopy. *Surf. Sci.* 291:39–46.

Hinterdorfer, P., F. Kienberger, A. Raab, H. J. Gruber, W. Baumgartner, G. Kada, C. Riener, S. Wielert-Badt, C. Borken, and H. Schindler. 2000. Poly(ethylene glycol): an ideal spacer for molecular recognition force microscopy/spectroscopy. *Single Mol.* 1:99–103.

Hutter, J. L., and J. Bechhoefer. 1993. Calibration of atomic force microscopy tips. *Rev. Sci. Instrum.* 64:1868–1873.

Ippolito, J. A., and T. A. Steitz. 1998. A 1.3 Å resolution crystal structure of the HIV-1 trans-activation response region RNA stem reveals a metal ion-dependent bulge conformation. *Proc. Natl. Acad. Sci. USA.* 95:9819–9824.

Krautbauer, R., L. H. Pope, T. E. Schrader, S. Allen, and H. E. Gaub. 2002. Discriminating drug-DNA binding modes by single molecule force spectroscopy. *FEBS Lett.* 510:154–158.

Leblanc, D. A., and K. M. Morden. 1991. Thermodynamic characterization of deoxyribooligonucleotide duplexes containing bulges. *Biochemistry.* 30:4042–4047.

Lee, G. U., D. A. Kidwell, and R. J. Colton. 1994. Sensing discrete streptavidin biotin interactions with atomic force microscopy. *Langmuir.* 10:354–357.

Liphardt, J., S. Dumont, S. B. Smith, I. Tinoco, Jr., and C. Bustamante. 2002. Equilibrium information from nonequilibrium measurements in an experimental test of Jarzynski's equality. *Science.* 296:1832–1835.

Liphardt, J., B. Onoa, S. B. Smith, I. Tinoco, Jr., and C. Bustamante. 2001. Reversible unfolding of single RNA molecules by mechanical force. *Science.* 292:733–737.

Longfellow, C. E., R. Kierzek, and D. H. Turner. 1990. Thermodynamic and spectroscopic study of bulge loops in oligoribonucleotides. *Biochemistry.* 29:278–285.

Mathews, D. H., J. Sabina, M. Zuker, and D. H. Turner. 1999. Expanded sequence dependence of thermodynamic parameters improves prediction of RNA secondary structure. *J. Mol. Biol.* 288:911–940.

Merkel, R., P. Nassoy, A. Leung, K. Ritchie, and E. Evans. 1999. Energy landscapes of receptor-ligand bonds explored with dynamic force spectroscopy. *Nature.* 397:50–53.

Moore, P. B. 1999. Structural motifs in RNA. *Annu. Rev. Biochem.* 68: 287–300.

Mukerji, I., and A. P. Williams. 2002. UV resonance Raman and circular dichromism studies of a DNA duplex containing an A_3T_3 tract: evidence for a pre-melting transition and three-centered H-bonds. *Biochemistry.* 41:69–77.

Noy, A., D. V. Vezenov, J. F. Kayyem, T. J. Meade, and C. M. Lieber. 1997. Stretching and breaking duplex DNA by chemical force. *Chem. Biol.* 4:519–527.

Onoa, B., S. Dumont, J. Liphardt, S. B. Smith, I. Tinoco, Jr., and C. Bustamante. 2003. Identifying kinetic barriers to mechanical unfolding of the *T. thermophila* ribozyme. *Science.* 299:1892–1895.

Pope, L. H., M. C. Davies, C. A. Laughton, C. J. Roberts, S. J. B. Tendler, and P. M. Williams. 2001. Force-induced melting of a short DNA double helix. *Eur. Biophys. J.* 30:53–62.

Pörschke, D. 1977. Elementary steps of base recognition and helix-coil transitions in nucleic acids. *Mol. Biol. Biochem. Biophys.* 24:191–218.

Press, W. H., S. A. Teukolsky, W. T. Vetterling, and B. P. Flannery. 1992. Numerical recipes in C. Cambridge University Press, New York.

Rief, M., H. Clausen-Schaumann, and H. E. Gaub. 1999. Sequence dependent mechanics of single DNA molecules. *Nat. Struct. Biol.* 6: 346–349.

Saenger, W. 1984. Principles of Nucleic Acid Structure. Springer Verlag, New York.

Schuler, B., E. A. Lipman, and W. A. Eaton. 2002. Probing the free-energy surface for protein folding with single molecule fluorescence spectroscopy. *Nature*. 419:743–747.

Schumakovitch, I., W. Grange, T. Strunz, P. Bertoncini, H.-J. Güntherodt, and M. Hegner. 2002. Temperature dependence of unbinding forces between complementary DNA strands. *Biophys. J.* 82:517–521.

Serra, M. J., J. D. Baird, T. Dale, B. T. Fey, K. Retatagos, and E. Westhof. 2002. Effects of magnesium ions on the stabilization of RNA oligomers of defined structures. *RNA*. 8:307–323.

Strunz, T., K. Oroszlan, R. Schäfer, and H.-J. Güntherodt. 1999. Dynamic force spectroscopy of single DNA molecules. *Proc. Natl. Acad. Sci. USA*. 96:11277–11282.

Ulanovsky, L. E., and E. N. Trifonov. 1987. Estimation of wedge components in curved DNA. *Nature*. 326:720–722.

Williams, P., and E. Evans. 2001. Dynamic force spectroscopy. II. Multiple bonds. *In* Les Houches Session LXXV Physics of Bio-Molecules and Cells. H. Flyvbjerg, F. Jülicher, P. Ormos, and F. David, editors. Springer-Verlag, Berlin. 187–204

Willemsen, O. H., M. M. E. Snel, K. O. van der Werf, B. G. de Grooth, J. Greve, P. Hinterdorfer, H. J. Gruber, H. Schindler, Y. van Kooyk, and C. G. Figdor. 1998. Simultaneous height and adhesion imaging of antibody-antigen interactions by atomic force microscopy. *Biophys. J.* 75:2220–2228.

Xia, T., J. SantaLucia, Jr., M. E. Burkard, R. Kierzek, S. J. Schroeder, X. Jiao, C. Cox, and D. H. Turner. 1998. Parameters for an expanded nearest-neighbour model for formation of RNA duplexes with Watson-Crick pairs. *Biochemistry*. 37:14719–14735.

Zacharias, M., and P. J. Hagerman. 1995. The bend in RNA created by the transactivation response element bulge of HIV is straightened by arginine and TAT-derived peptide. *Proc. Natl. Acad. Sci. USA*. 92:6052–6056.

Zagórowska, I., and R. W. Adamiak. 1996. 2-aminopurine labelled RNA bulge loops. Synthesis and thermodynamics. *Biochimie*. 78:123–130.

Zhuang, X., L. E. Bartley, H. P. Babcock, R. Russell, T. Ha, D. Herschlag, and S. Chu. 2000. A single-molecule study of RNA catalysis and folding. *Science*. 288:2048–2051.